

Cite this: *Chem. Sci.*, 2020, 11, 6485

All publication charges for this article have been paid for by the Royal Society of Chemistry

Received 3rd March 2020  
Accepted 13th April 2020

DOI: 10.1039/d0sc01291b

rsc.li/chemical-science

# Cationic indium catalysts for ring opening polymerization: tuning reactivity with hemilabile ligands†

Chatura Goonesinghe, Hootan Roshandel, Carlos Diaz, Hyuk-Joon Jung, Kudzanai Nyamayaro, Maria Ezhova and Parisa Mehrkhodavandi\*

This is a comprehensive study of the effects of rationally designed hemilabile ligands on the stability, reactivity, and change in catalytic behavior of indium complexes. We report cationic alkyl indium complexes supported by a family of hemi-salen type ligands bearing hemilabile thiophenyl (2a), furfuryl (2b) and pyridyl (2c) pendant donor arms. Shelf-life and stability of these complexes followed the trend  $2a < 2b < 2c$ , showing direct correlation to the affinity of the pendant donor group to the indium center. Reactivity towards polymerization of epichlorohydrin and cyclohexene oxide followed the trend  $2a > 2b > 2c$  with control of polymerization following an inverse relationship to reactivity. Surprisingly, **2c** polymerized *racemic* lactide without an external initiator, likely through an alkyl-initiated coordination-insertion mechanism.

## Introduction

Hemilabile ligands have been extensively used to stabilize metal complexes, and control and even alter reactivity.<sup>1</sup> A wide array of elegant hemilabile ligand architectures support transition metal centers with catalytic activity in processes such as carbonylation,<sup>2</sup> alkylation,<sup>3</sup> amination,<sup>4</sup> cross-coupling,<sup>5</sup> and olefin metathesis<sup>6</sup> among others.<sup>7</sup>

In contrast, there are only a handful of reports of the use of hemilabile ligands with main group metals.<sup>8</sup> Due to their tunable Lewis acidity and oxophilic nature, complexes of group 13 elements, especially aluminum<sup>9</sup> and indium<sup>10</sup> have been used in a variety of reactions ranging from ring opening polymerization (ROP) of cyclic polar monomers to functionalization of small molecules.<sup>11</sup> However, among the group 13 metals, almost all reports<sup>12</sup> focus on aluminum complexes (Chart 1).

In cationic aluminum complexes, hemilabile ligands have been used for stabilizing complexes. The first group 13 complexes bearing hemilabile ligands to show reactivity were reported by Dagorne and co-workers.<sup>13</sup> These cationic aluminum complexes, **A**, bearing piperazine and morpholine pendant arms, stabilized the cationic center and showed catalytic reactivity for the ROP of propylene oxide. Kerton and co-workers reported the ROP of  $\epsilon$ -caprolactone ( $\epsilon$ -CL) using

a cationic aluminum complex **B**, stabilized by a morpholinyl donor arm.<sup>14</sup> Another cationic aluminum complex, **C**, proposed to be stabilized by two hemilabile furfuryl pendant arms was reported by Phomphrai and co-workers.<sup>15</sup>

Control of reactivity using hemilability was demonstrated by Shaver and co-workers by showing that the coordination of various donor arms to an aluminum center in a series of complexes, **D**, was key to obtaining control in the ROP of *racemic*

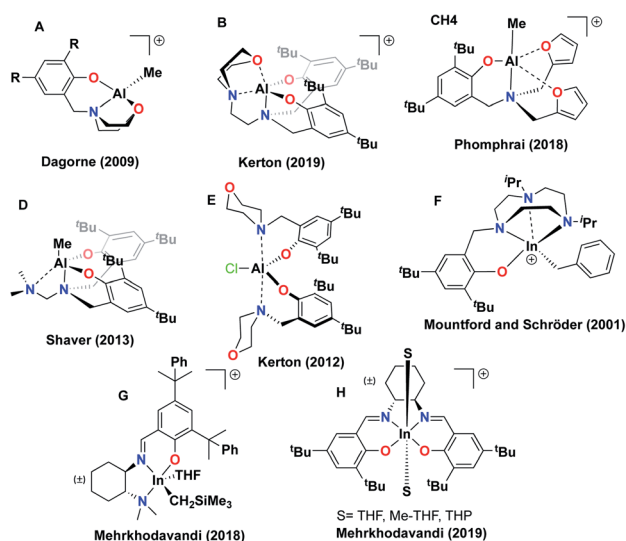


Chart 1 Previously reported aluminum and indium complexes bearing hemilabile ligands (A–F) and cationic indium complexes reported by our group (G and H).

Department of Chemistry, University of British Columbia, Vancouver, BC, Canada.  
E-mail: mehr@chem.ubc.ca

† Electronic supplementary information (ESI) available: Experimental procedures, solution and solid-state characterization. CCDC 1987632–1987636. For ESI and crystallographic data in CIF or other electronic format see DOI: 10.1039/d0sc01291b



lactide (*rac*-LA) and  $\epsilon$ -CL.<sup>16</sup> Finally, Kerton and co-workers reported an example of hemilabile donors altering reactivity in aluminum complexes. They showed that the displacement of an ancillary chloride ligand was facilitated by a hemilabile pendant arm in a neutral complex, **E**, to initiate the (co)polymerization of CO<sub>2</sub> and cyclohexene oxide (CHO).

To the best of our knowledge, the first indium complexes bearing a hemilabile ligand architecture investigated for reactivity were described by Mountford who reported an indium alkyl complex supported by an aminophenolate ligand with a 1,4,7-triazacyclononane hemilabile pendant arm (**F**); their complex was unreactive towards all nucleophiles and reagents examined.<sup>17</sup> We have reported indium catalysts supported by tridentate<sup>18</sup> and tetradentate<sup>19</sup> amino/imino phenolate ligands as catalysts for ROP reactions. However, due to their increased electrophilicity and coordinative unsaturation, we have recently focused on studying cationic complexes for the coupling of epoxides and  $\epsilon$ -CL to form spiroorthoesters (**G**)<sup>20</sup> and the copolymerization of cyclic ethers and lactide (**H**).<sup>21</sup> However, both these complexes required solvent molecules for stabilization, and the isolated complexes suffered from rapid decomposition when the labile solvent molecules were lost. We proposed that a ligand architecture with a hemilabile pendant donor moiety could stabilize the cationic indium center, afford greater control of reactivity, and potentially change the reactivity pattern altogether.

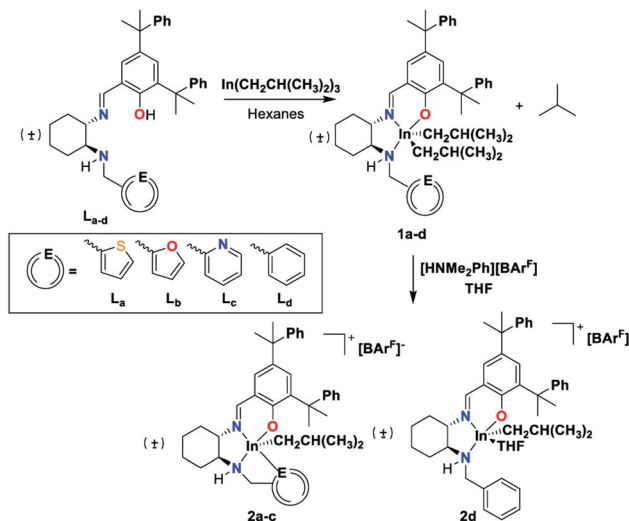
Herein, we report the first catalytically active cationic alkyl indium complexes supported by ligands bearing hemilabile pendant donor arms with varying donor strengths. We show the pendant donor groups can be used to tune the stability of the cationic alkyl indium complexes. Furthermore, we show that these complexes can be used to control the ROP reactivity of epichlorohydrin and cyclohexene oxide. Finally, we observe that the reactivity of the cationic alkyl indium center towards ROP of *rac*-LA is radically altered in the presence of a strong donor group, allowing alkyl initiated polymerization. This is the first example of using rationally designed hemilabile ligands to tune the reactivity of indium complexes.

## Results and discussion

### Synthesis and characterization of complexes

The proligands (**L<sub>a-d</sub>**) can be synthesized using modified literature procedures<sup>22</sup> from ( $\pm$ )-*trans*-1,2-diaminocyclohexane and 2-carbaldehydes of thiophene (**L<sub>a</sub>**), furan (**L<sub>b</sub>**), pyridine (**L<sub>c</sub>**), and benzene (**L<sub>d</sub>**) (see ESI<sup>†</sup>). Reactions of **L<sub>a-d</sub>** with In(<sup>t</sup>Bu)<sub>3</sub> at room temperature forms indium dialkyl complexes [**L<sub>a-d</sub>**]In<sup>t</sup>Bu<sub>2</sub> (**1a-d**) (Scheme 1). **L<sub>d</sub>** was synthesized as a control to approximate the steric bulk of the donor arms in **L<sub>a-c</sub>** without the donating ability.

Solid-state structures of **1a-d** determined by single-crystal X-ray crystallography feature distorted square pyramidal indium centers (Fig. S57–S60<sup>†</sup>). All the dialkyl species are isostructural in the solid state, with the equivalent distances between the hemilabile arm heteroatoms and the indium center in **1a-c** indicating the absence of significant interactions. This is most apparent in comparison of this distance in **1c** and the



Scheme 1 Synthesis of neutral and cationic alkyl indium complexes.

analogous distance to the indium center from the *ortho*-C of the benzyl group in **1d**, where no interaction is expected (Fig. 1).

To determine donor group interaction in the solution-state for complexes **1a-d**, we used a modified Gutmann–Beckett method to determine relative acceptor ability (Fig. 2).<sup>23</sup> This method involves the addition of triethylphosphine oxide (OPET<sub>3</sub>) to form an adduct with the metal complex. Complexes **1a-d** did not show a significant change in <sup>31</sup>P{<sup>1</sup>H} chemical shifts relative to free OPET<sub>3</sub>, indicating that the indium centers of **1a-d** have electronically similar environments. This excludes the possibility of donor group interaction in the solution-state. The <sup>1</sup>H and <sup>13</sup>C{<sup>1</sup>H} NMR spectra obtained for **1a-d** in CDCl<sub>3</sub> agree with the solid-state structures (Fig. S17–S35<sup>†</sup>).

The reaction of complexes **1a-d** with [HNMe<sub>2</sub>Ph][BARF] (BARF = tetrakis[3,5-bis(trifluoromethyl)phenyl]borate) in THF forms the cationic species **2a-d** (Scheme 1). The stability of the complexes in the absence of donor solvents is related to the affinity of the heteroatom to the indium center (Table S1<sup>†</sup>). Complexes **2a-c** can be synthesized in non-coordinating solvents such as dichloromethane and benzene, while **2d** formed decomposition products under these conditions.

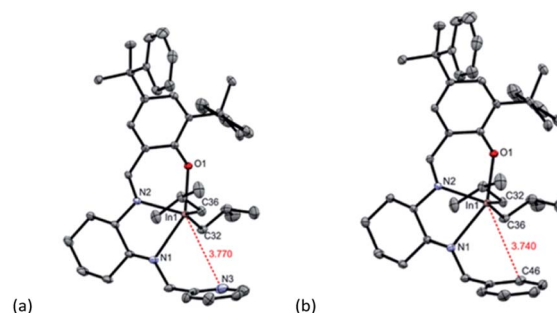


Fig. 1 Molecular structures of complex (a) [**L<sub>c</sub>**]In<sup>t</sup>Bu<sub>2</sub> (**1c**) and (b) [**L<sub>d</sub>**]In<sup>t</sup>Bu<sub>2</sub> (**1d**) (depicted with thermal ellipsoids at 50% probability and H atoms, as well as solvent molecules omitted for clarity).



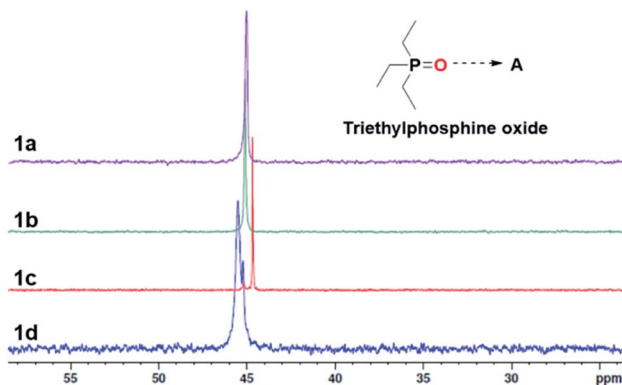


Fig. 2  $^{31}\text{P}\{^1\text{H}\}$  NMR spectra of  $\text{OPEt}_3$  with **1a–d** show a similar acceptor ability for neutral complexes.  $^{31}\text{P}\{^1\text{H}\}$  NMR (160 MHz,  $\text{C}_6\text{H}_6$ , 25 °C) chemical shift of free  $\text{OPEt}_3$  appears at 45 ppm.

Complex **2d** could be synthesized at  $-30$  °C in THF but was not isolable with high purity. After several hexane washes, residual THF can be removed from complexes **2a–c**, while for complex **2d** THF cannot be removed. This is reminiscent of the similar alkyl indium cationic catalyst **G** (Chart 1).<sup>20</sup>

The  $^1\text{H}$  NMR signals arising from the heterocyclic protons in **2a–c** shift significantly upfield compared to the neutral species **1a–c**, suggesting substantial shielding of these protons upon formation of the cationic complexes. Further analysis of the  $^1\text{H}$  NMR spectrum of **2c** shows that the AB multiplet ( $\nu < 10$  J) arising from the diastereotopic methylene protons of the pendant arm broaden and shift downfield by  $\sim 0.2$  ppm compared to **1c**. In **2a**, and to a lesser extent in **2b**, the  $\Delta\delta$  for these protons increase, in relation to **1a** and **1b**, resembling an AX coupling ( $\nu \geq 10$  J, Fig. 3). Based on these observations, we propose that the upfield shift of heterocyclic proton signals arise when the outer-sphere donor group approaches the cationic indium center, enhancing shielding of the heterocyclic protons. Coordination of the pendant donor groups to the cationic center would restrict the free rotation around the methylene carbon on the linker arm, thereby “locking” the methylene protons in position and increasing the  $\Delta\delta$  of these protons.

NOESY NMR spectra of **1a–c** showed no through space interaction between heterocyclic protons and isobutyl protons

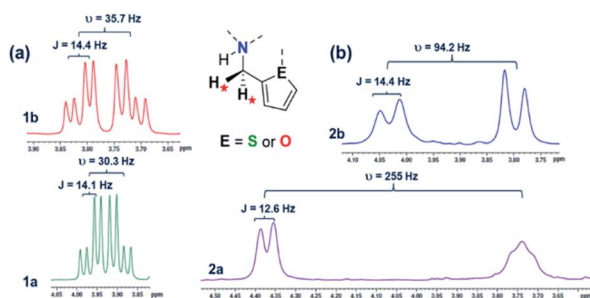


Fig. 3 (a) Methylene protons ( $\text{H}_*$ ) are an AB pair in **1a** and **1b**. (b) In **2a** and **2b** they act like an AX pair ( $^1\text{H}$  NMR at 300 MHz in  $\text{CDCl}_3$  at 25 °C).

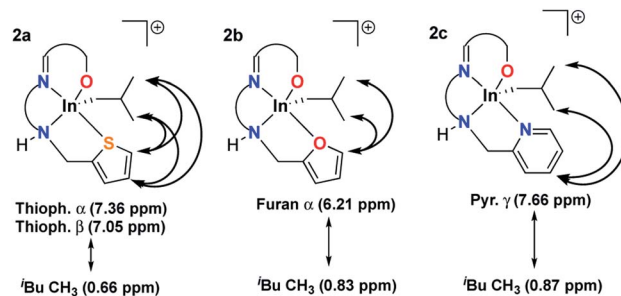


Fig. 4 Significant through space interactions between heterocyclic protons and methyl protons of the isobutyl ligand (NOESY NMR spectra 400 MHz,  $\text{CDCl}_3$ , 25 °C).

(Fig. S21, S26 and S31<sup>†</sup>). However, heterocyclic protons on **2a–c** show NOE interactions with the methyl protons of the isobutyl ligands (Fig. S40, S47 and S54<sup>†</sup>) indicating increased proximity of the pendant donor groups to the isobutyl methyl groups through the coordination of the side arms (Fig. 4).

### Hemilabile behavior of complexes

In previously reported studies with aluminum complexes bearing hemilabile ligands, temperature was a defining factor in complex stability and reactivity. At high temperatures, Phomphrai and co-workers reported the decomposition of cationic aluminum complex **E**, while Shaver and co-workers reported a loss of control in polymerization of  $\epsilon$ -CL with complex **C** (Chart 1).<sup>15,16</sup> It is likely that decomposition or loss of control occurs with the de-coordination of hemilabile groups at these higher temperatures.

Variable temperature (VT)  $^1\text{H}$  NMR spectroscopy (25–125 °C,  $\text{C}_6\text{D}_5\text{Br}$ ) of cationic complexes **2a–c** show significant changes, while the neutral analogues do not change in this temperature range (Fig. S63–S65<sup>†</sup>). The thiophene complex **2a** shows significant and irreversible decomposition beginning at 45 °C, while the pyridyl complex **2c** was highly stable, with only minor changes in chemical shifts even at 120 °C. In contrast, the furan complex **2b** shows a gradual downfield migration of the  $\alpha$  furfuryl proton with increasing temperature, a  $\Delta\delta$  of  $\sim 0.6$  ppm (Fig. 5). At higher temperatures (125 °C,  $\text{C}_6\text{D}_5\text{Br}$ ) the chemical shift of the  $\alpha$  proton approaches that of the free ligand ( $\delta = 7.20$

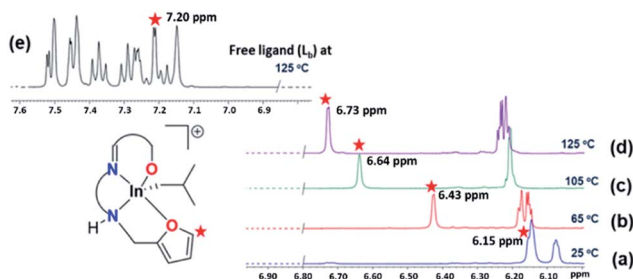


Fig. 5 (a–d) VT  $^1\text{H}$  NMR (400 MHz,  $\text{C}_6\text{D}_5\text{Br}$ , 25–125 °C) spectra showing downfield migration of the  $\alpha$  proton of the furfuryl group ( $*$ ) in **2b**. (e) Spectrum of the free ligand ( $\text{L}_b$ ) at 125 °C.



ppm). This change is reversible when the temperature is lowered to 30 °C.

We propose that the de-shielding of the  $\alpha$  proton occurs as its proximity to the indium center decreases with increasing fluxional behavior of the In–O<sub>furan</sub> interaction at higher temperatures. This behavior of **2a–c** is directly related to the donor ability of the heterocyclic pendant groups. The greater donor ability of pyridine (donor strength,  $D_S = 38$ ) compared to furan and thiophene ( $D_S = 11$  and 10, respectively) accounts for the unexpected stability of **2c**.<sup>24</sup> However, donor strength alone does not explain the dramatic difference in stability between **2a** and **2b**. The higher stability of **2b** can be accounted for by the greater aromaticity of thiophene and the availability of electrons in furan for bonding.<sup>25</sup>

For these complexes to be truly hemilabile, the pendant donor arm must change its bonding in response to other coordinating ligands or solvent molecules possessing a greater donor ability.<sup>14</sup> We studied the hemilabile behavior of furan substituted **2b** in detail due to its “Goldilocks” stability and the easily observable  $\alpha$ -proton chemical shift in the <sup>1</sup>H NMR spectra (Fig. 6). With the addition of THF ( $D_S = 17$ ) to **2b**, a  $\sim 0.5$  ppm downfield shift of the  $\alpha$ -proton signal was observed in the <sup>1</sup>H NMR spectrum (C<sub>6</sub>D<sub>6</sub>) of the mixture, indicating a loss of proximity of the furan moiety (Fig. 6b). With a weaker donor such as epichlorohydrin (ECH), only a  $\sim 0.1$  ppm downfield shift is observed, while addition of pyridine ( $D_S = 38$ , donor number  $D_N = 33.1$ )<sup>26</sup> causes a  $\sim 0.6$  ppm downfield shift. Addition of OPET<sub>3</sub> had the greatest effect with a  $\sim 0.9$  ppm downfield shift (Fig. 6d). While, OPET<sub>3</sub> has a lower donor number ( $D_N = 24$ ) than pyridine, the predominantly anionic nature of the oxygen leads to a stronger interaction with the cationic indium center and a greater fluxionality of the In–O<sub>furan</sub> interaction.<sup>27</sup>

A single-crystal of solvated **2b**·2THF suitable for single crystal X-ray crystallographic analysis was obtained through the slow evaporation of a THF/hexamethyldisiloxane solution. The structure of **2b**·2THF revealed a distorted octahedral indium center with THF molecules in the axial position (Fig. 7). The bond distances and angles of **2b**·2THF resemble those of cationic salen indium complex **H** (Chart 1).<sup>21</sup> The de-coordination of the furfuryl pendant arm in the presence of an external donor entity confirms that **2b** displays true hemilabile behavior.

Although the solid-state structure of **2b**·2THF shows the coordination of two THF molecules and the complete de-coordination of the pendant donor arm, the structure is

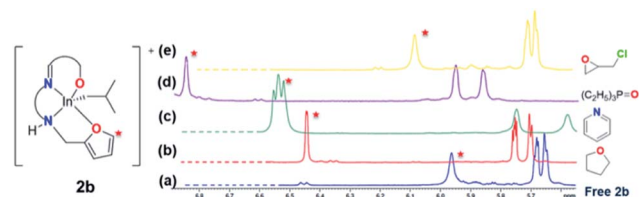


Fig. 6 <sup>1</sup>H NMR (400 MHz, C<sub>6</sub>D<sub>6</sub>, 25 °C) downfield shift of the furfuryl  $\alpha$  proton signal (\*) of **2b** in the presence of (b) THF, (c) pyridine, (d) triethylphosphine oxide and (e) epichlorohydrin.

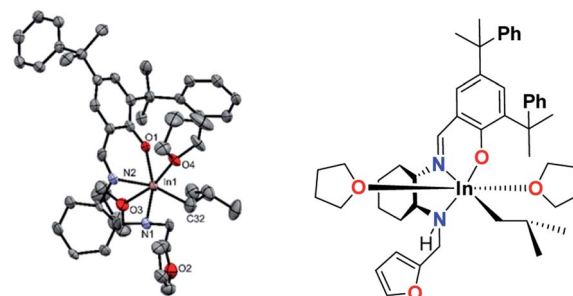


Fig. 7 Molecular structures of complex **2b**·2THF (depicted with thermal ellipsoids at 50% probability and H atoms, minor disorders as well as solvent molecules and counter anion omitted for clarity).

different in solution. The DOSY NMR spectrum (C<sub>6</sub>D<sub>6</sub>) exhibits independent diffusion of **2b** and THF (Fig. 8). These results point to a weak association of **2b** with THF in solution phase. This observation held true for DOSY NMR of mixtures of **2a** and **2c** with THF as well (Fig. S70 and S72†). It is possible that this apparent independent diffusion of the complexes and THF is due to fast exchange occurring relative to the NMR time scale at 25 °C at 400 MHz.

### Polymerization of epoxides

The cationic ring opening polymerization (ROP) of epichlorohydrin (ECH) in C<sub>6</sub>D<sub>6</sub> was used as a model reaction to determine the effect of hemilabile donor groups on reactivity and the polymers were characterized by gel permeation chromatography (GPC, Table 1). Complex **2d**, which lacks a donor arm, shows the highest activity at 25 °C with an initiation efficiency (percentage of catalyst initiating polymerization)<sup>28</sup> of 99%, while complex **2c** with the strong pyridine donor arm does not polymerize ECH even at 80 °C.

Complexes **2a** and **2b** catalyze the ROP of ECH at 25 °C with 61% and 39% initiation efficiencies, respectively. The initiation efficiency of **2b** approaches that of **2a** at higher temperatures indicating that both complexes achieve similar reactivity at elevated temperatures. Additionally, when triphenylphosphine is added to the reaction mixture, polymerization of the epoxide halts due to the formation of a stable quaternary phosphonium species at the cationic chain end.<sup>29</sup> This confirms the cationic

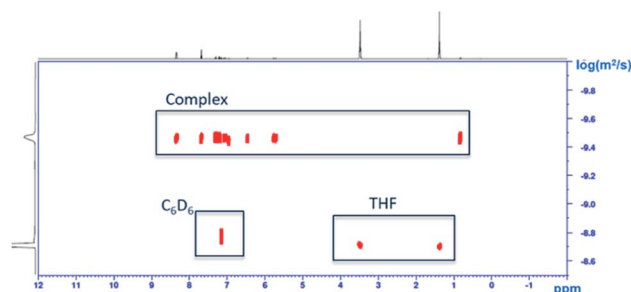
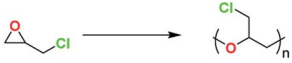


Fig. 8 DOSY NMR spectrum of **2b** with excess THF (<sup>1</sup>H NMR, diffusion time ( $\Delta$ ) = 0.85 s, gradient length ( $\delta$ ) = 400  $\mu$ s, 400 MHz, C<sub>6</sub>D<sub>6</sub>, 25 °C).



Table 1 Polymerization of epichlorohydrin with cationic alkyl indium complexes<sup>a</sup>


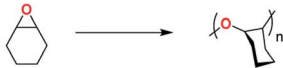
	Temp. (°C)	Cat.	Conv. <sup>b</sup> (%)	$M_{n \text{ Cal}}^c$ (Da)	$M_n^d$ (Da)	$D^e$	$i^{*f}$ (%)
1	25	2a	59	16 900	27 000	1.42	61
2	35	2a	61	16 900	21 300	1.56	80
3	60	2a	59	16 400	19 300	1.22	85
4 <sup>g</sup>	25	2a	<1	—	—	—	—
5 <sup>h</sup>	25	2a	<1	—	—	—	—
6	25	2b	34	9400	24 000	1.23	39
7	35	2b	61	16 900	29 300	1.33	58
8	60	2b	55	15 300	21 200	1.30	72
9 <sup>g</sup>	25	2b	<1	—	—	—	—
10 <sup>h</sup>	25	2b	<1	—	—	—	—
11	25	2c	<1	—	—	—	—
12	60	2c	<1	—	—	—	—
13	80	2c	<1	—	—	—	—
14 <sup>i</sup>	25	2d	73	20 400	20 500	1.50	99

<sup>a</sup> Reactions were performed in C<sub>6</sub>D<sub>6</sub> for 24 h. [ECH] = 6.37 M, [cat] = 20 mM. [ECH]/[cat] = 300. <sup>b</sup> Conversion was monitored by <sup>1</sup>H NMR spectroscopy. <sup>c</sup>  $M_{n \text{ Cal}}$  = calculated number averaged molecular weight = [ECH]/[cat] × conversion × molar mass of ECH. <sup>d</sup>  $M_n$  determined using GPC in THF. <sup>e</sup> Dispersity =  $M_w/M_n$ . <sup>f</sup> Initiation efficiency =  $(M_{n \text{ Cal}}/M_n) \times 100$ . <sup>g</sup> With the addition of triphenylphosphine. <sup>h</sup> [ECH] = 2.94 M, [cat] = 10 mM, [ECH]/[cat] = 300. <sup>i</sup> Catalyst was not isolable.

nature of the polymerization mechanism (Table 1, entries 4 and 9).

The polymerization of highly reactive cyclohexene oxide (CHO)<sup>30</sup> provides a dramatic example of the tuning of reactivity through the introduction of a hemilabile donor arm. Under neat, dilute, and even low temperature conditions, **2a** and **2b** polymerize CHO in an uncontrolled fashion, forming polymers with high dispersity and irreproducible molecular weights

(Table 2, entries 1–6). In contrast to these species, **2c** reacts slowly to produce higher molecular weight, lower dispersity poly(cyclohexene oxide) even in neat conditions. Reactions carried out at a higher temperature show greater conversions, while those carried out in solution show increased molecular weights with a significant lowering of dispersity (Table 2, entries 7–9). Although **2c** is not highly controlled in general, this change in reactivity clearly shows the significant impact of the hemilabile arm.

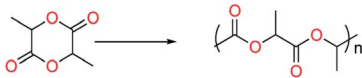
Table 2 Polymerization of cyclohexene oxide with cationic alkyl indium complexes<sup>a</sup>


	Temp. (°C)	Cat.	Solv.	Conv. <sup>b</sup> (%)	$M_{n \text{ Cal}}^c$ (Da)	$M_n^d$ (Da)	$D^e$
1	25	2a	Neat	*	—	~13 000	~7
2	25	2a	C <sub>6</sub> D <sub>6</sub>	*	—	~20 000	~4
3	0	2a	Tol.	*	—	~19 000	~3
4	25	2b	Neat	*	—	~14 000	~5
5	25	2b	C <sub>6</sub> D <sub>6</sub>	*	—	~30 000	~3
6	0	2b	Tole	*	—	~24 000	~3
7	25	2c	Neat	58	113 800	80 800	2.23
8	60	2c	Neat	93	182 500	82 800	1.78
9	25	2c	C <sub>6</sub> D <sub>6</sub>	91	26 800	108 600	1.47
10 <sup>f</sup>	25	2c	Neat	—	—	—	—

<sup>a</sup> Reactions were performed for 24 h. In solution [CHO] = 8.0 M, [cat] = 5.6 mM. [Epoxide]/[cat] = 300, in neat conditions [epoxide]/[cat] = 2000. <sup>b</sup> Conversion was monitored by <sup>1</sup>H NMR spectroscopy. <sup>c</sup>  $M_{n \text{ Cal}}$  = calculated number averaged molecular weight = [CHO]/[cat] × conversion × molar mass of CHO. <sup>d</sup>  $M_n$  determined using GPC in THF. <sup>e</sup> Dispersity =  $M_w/M_n$ . <sup>f</sup> With the addition of triphenylphosphine. \*Not determined due to uncontrolled reaction.

### Polymerization of racemic lactide (*rac*-LA)

The ROP of *rac*-LA does not proceed through a cationic mechanism (Table 3). Under the reaction conditions **2a** did not polymerize *rac*-LA while **2b** showed <20% conversion of

Table 3 Polymerization of racemic lactide with cationic alkyl indium complexes<sup>a</sup>


	Catalyst	Conv. <sup>b</sup> (%)	$M_{n \text{ Cal}}^c$ (Da)	$M_n^d$ (Da)	$D^e$	$i^{*f}$ (%)
1	2a	<1	—	—	—	—
2	2b	20	—	—	—	—
3	2c	94	34 000	130 000	1.32	26

<sup>a</sup> Reactions were performed for 24 h in toluene at 100 °C. [*rac*-LA] = 1.6 M, [cat] = 6.4 mM. [*rac*-LA]/[cat] = 250. <sup>b</sup> Conversion was monitored by <sup>1</sup>H NMR spectroscopy. <sup>c</sup>  $M_{n \text{ Cal}}$  = calculated number averaged molecular weight = [*rac*-LA]/[cat] × conversion × molar mass of *rac*-LA. <sup>d</sup>  $M_n$  determined through GPC in THF. <sup>e</sup> Dispersity =  $M_w/M_n$ . <sup>f</sup> Initiation efficiency =  $(M_{n \text{ Cal}}/M_n) \times 100$ .



monomer. Possibly due to the formation of low molecular weight oligomers, the products could not be isolated. In contrast, **2c** produced high molecular weight, low dispersity polymer with high conversion.

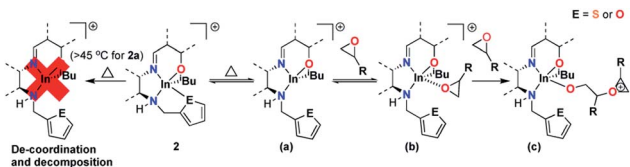
The polymerization of *rac*-LA in the absence of an external initiator by **2c** is unexpected. Analysis of the resultant polymer by MALDI-TOF mass spectrometry (MS) indicates that the polymerization is initiated by the In–isobutyl moiety (Fig. S74†). While there have been reports of neutral indium and rare-earth alkyl species capable of initiating ROP of *rac*-LA with an alkyl group,<sup>31</sup> to the best of our knowledge, **2c** is the first cationic metal complex to do so. In complex **G**, we found that the alkyl group attached to the cationic indium center is very stable even in the presence of trace amounts of water.<sup>20</sup> However, in **2c** and to a lesser extent in **2b**, the electrophilicity of the indium center is decreased through the coordination of the hemilabile donor arm, weakening the In–C bond. We propose that with the presence of a strong hemilabile donor, the lability of the isobutyl group increases allowing it to act as an initiator in the polymerization of *rac*-LA.

### Mechanistic considerations

Based on the experiments above, we can propose two contrasting mechanisms for the ROP of epoxides and *rac*-LA with catalysts **2a–c**. As the controlled ROP of CHO is limited to complex **2c**, we will use ECH as a model to discuss reactivity patterns (Scheme 2). The ROP of ECH proceeds *via* a cationic mechanism, in which the role of the catalyst is limited to the initiation step and is reflected in the initiation efficiency of the catalysts. Initiation requires the extensive dissociation of the hemilabile donor, therefore complex **2c** is not active for the ROP of ECH.

For complex **2b**, the donor arm dissociates reversibly, with more pronounced fluxional behavior of the In–O<sub>furan</sub> bond with increasing temperatures. This facilitates the coordination of epoxide, resulting in higher initiation efficiencies at elevated temperatures (Scheme 2a and b). At these temperatures the dissociation of the pendant arm for **2a** is not reversible and it decomposes in the absence of donors (monomers or solvent).

Monomer concentration also affects initiation efficiencies. At low [ECH] the monomer coordinates to the cationic center reversibly; however, under these conditions, polymerization does not proceed (Table 1, entries 5 and 10). At higher [ECH] polymerization is initiated, and propagation ensues with the attack by a second epoxide molecule (Scheme 2c).



Scheme 2 Proposed behavior of cationic complexes with (a) increasing temperature, (b) in the presence of a low concentration of epoxide and (c) at high concentration of epoxide resulting in cationic polymerization.

In contrast, we propose that *rac*-LA is polymerized through an alkyl-initiated coordination-insertion mechanism. This requires a highly activated In–C bond, which is not present in complexes **2a**, **2b**, or **G**. Complex **2c** is active because of the greater donor ability of the pyridyl group, which decreases the electrophilicity of the indium center, polarizing the In–C bond. The difference in reactivity towards the ROP of *rac*-LA under the same conditions shows the clear influence the donor arm has on the reactive behavior of the complexes. This represents a rare example of changing reactivity patterns using a hemilabile donor group.

## Conclusions

In this study we show that the donor ability of the heterocyclic moiety on ligand supports for cationic indium complexes profoundly affects the labile behavior of the pendant donor arms, and thus impacts the stability and the reactivity of the complexes. Through the addition of the hemilabile donor groups, we were able to achieve the following outcomes:

First, the complex stability and shelf life was significantly improved in hemilabile ligand bearing complexes **2a–c** relative to the solvent stabilized **2d**. The stability followed a trend with a direct correlation of complex stability to the donor ability of the pendant groups (**2d** < **2a** < **2b** < **2c**).

Second, the reactivity could be controlled by regulating the coordination of reactants to the indium center. The reactivity is inversely related to stability with **2a** and **2b**, both of which are active for the ROP of epichlorohydrin. Unusually for a cationic species, **2c** showed controlled reactivity towards ROP of CHO in neat conditions. The ROP of epoxides provides proof of reactivity control enforced by the hemilabile ligand system.

Third, typical reactivity of cationic alkyl indium complexes was altered by the addition of the pyridyl pendant group in **2c**. Complex **2c** was capable of alkyl initiated ROP of *rac*-LA through a coordination insertion mechanism. This provides an example of altering reactivity at the metal center by a hemilabile ligand system.

We aim to use our studies in furthering reactivity with cationic indium complexes.

## Conflicts of interest

There are no conflicts to declare.

## Acknowledgements

The authors acknowledge the Natural Sciences and Engineering Council of Canada (NSERC) for funding this work.

## References

- (a) C. S. Slone, D. A. Weinberger and C. A. Mirkin, *Prog. Inorg. Chem.*, 1999, **48**, 233–350; (b) P. Braunstein and F. Naud, *Angew. Chem., Int. Ed.*, 2001, **40**, 680–699.
- (a) K. W. Dong, R. Sang, Z. H. Wei, J. Liu, R. Dühren, A. Spannenberg, H. J. Jiao, H. Neumann, R. Jackstell,



- R. Franke and M. Beller, *Chem. Sci.*, 2018, **9**, 2510–2516; (b) K. Tanaka, W. R. Ewing and J. Q. Yu, *J. Am. Chem. Soc.*, 2019, **141**, 15494–15497.
- 3 P. M. P. Garcia, P. Ren, R. Scopelliti and X. L. Hu, *ACS Catal.*, 2015, **5**, 1164–1171.
- 4 M. V. Jimenez, J. J. Perez-Torrente, M. I. Bartolome, F. J. Lahoz and L. A. Oro, *Chem. Commun.*, 2010, **46**, 5322–5324.
- 5 (a) S. Handa, J. D. Smith, M. S. Hageman, M. Gonzalez and B. H. Lipshutz, *ACS Catal.*, 2016, **6**, 8179–8183; (b) Z. Q. Weng, S. H. Teo and T. S. A. Hor, *Acc. Chem. Res.*, 2007, **40**, 676–684.
- 6 C. S. Higman, D. L. Nascirmento, B. J. Ireland, S. Audorsch, G. A. Bailey, R. McDonald and D. E. Fogg, *J. Am. Chem. Soc.*, 2018, **140**, 1604–1607.
- 7 (a) H. F. Cheng, A. I. d'Aquino, J. Barroso-Flores and C. A. Mirkin, *J. Am. Chem. Soc.*, 2018, **140**, 14590–14594; (b) E. B. Hulley, M. L. Helm and R. M. Bullock, *Chem. Sci.*, 2014, **5**, 4729–4741; (c) M. S. Rosen, C. L. Stern and C. A. Mirkin, *Chem. Sci.*, 2013, **4**, 4193–4198.
- 8 (a) M. A. Dureen and D. W. Stephan, *Dalton Trans.*, 2008, 4723–4731; (b) G. L. Fondong, E. Y. Njua, A. Steiner, C. F. Campana and L. Stahl, *Polyhedron*, 2011, **30**, 2856–2862; (c) C. Gallegos, R. Camacho, M. Valiente, T. Cuenca and J. Cano, *Catal. Sci. Technol.*, 2016, **6**, 5134–5143; (d) I. Objartel, H. Ott and D. Stalke, *Z. Anorg. Allg. Chem.*, 2008, **634**, 2373–2379.
- 9 (a) N. Ikpo, S. M. Barbon, M. W. Drover, L. N. Dawe and F. M. Kerton, *Organometallics*, 2012, **31**, 8145–8158; (b) H. Plommer, I. Reim and F. M. Kerton, *Dalton Trans.*, 2015, **44**, 12098–12102.
- 10 (a) K. M. Osten and P. Mehrkhodavandi, *Acc. Chem. Res.*, 2017, **50**, 2861–2869; (b) A. Thevenon, A. Cyriac, D. Myers, A. J. P. White, C. B. Durr and C. K. Williams, *J. Am. Chem. Soc.*, 2018, **140**, 6893–6903.
- 11 (a) S. Dagorne, M. Normand, E. Kirillov and J. F. Carpentier, *Coord. Chem. Rev.*, 2013, **257**, 1869–1886; (b) S. Dagorne and R. Wehmschulte, *ChemCatChem*, 2018, **10**, 2509–2520; (c) Y. Sarazin and J. F. Carpentier, *Chem. Rev.*, 2015, **115**, 3564–3614; (d) J. H. Gao, D. Z. Zhu, W. J. Zhang, G. A. Solan, Y. P. Ma and W. H. Sun, *Inorg. Chem. Front.*, 2019, **6**, 2619–2652.
- 12 A. Arnold, T. J. Sherbow, R. I. Sayler, R. D. Britt, E. J. Thompson, M. T. Munoz, J. C. Fettinger and L. A. Berben, *J. Am. Chem. Soc.*, 2019, **141**, 15792–15803.
- 13 J. T. Issenhuth, J. Pluvinaige, R. Welter, S. Bellemin-Laponnaz and S. Dagorne, *Eur. J. Inorg. Chem.*, 2009, **31**, 4701–4709.
- 14 H. Plommer, J. N. Murphy, L. N. Dawe and F. M. Kerton, *Inorg. Chem.*, 2019, **58**, 5253–5264.
- 15 J. Kiriratnikom, S. Chotchatchawankul, S. Haesuwannakij, S. Kiatisevi and K. Phomphrai, *New J. Chem.*, 2018, **42**, 8374–8383.
- 16 E. D. Cross, G. K. Tennekone, A. Decken and M. P. Shaver, *Green Mater.*, 2013, **1**, 79–86.
- 17 D. A. Robson, S. Y. Bylikin, M. Cantuel, N. A. H. Male, L. H. Rees, P. Mountford and M. Schroder, *J. Chem. Soc., Dalton Trans.*, 2001, 157–169.
- 18 (a) A. F. Douglas, B. O. Patrick and P. Mehrkhodavandi, *Angew. Chem., Int. Ed.*, 2008, **47**, 2290–2293; (b) K. M. Osten, I. Yu, I. R. Duffy, P. O. Lagaditis, J. C. C. Yu, C. J. Wallis and P. Mehrkhodavandi, *Dalton Trans.*, 2012, **41**, 8123–8134; (c) C. Xu, I. Yu and P. Mehrkhodavandi, *Chem. Commun.*, 2012, **48**, 6806–6808; (d) I. Yu, A. Acosta-Ramirez and P. Mehrkhodavandi, *J. Am. Chem. Soc.*, 2012, **134**, 12758–12773; (e) K. M. Osten, D. C. Aluthge and P. Mehrkhodavandi, *Dalton Trans.*, 2015, **44**, 6126–6139; (f) I. Yu, T. Ebrahimi, S. G. Hatzikiriakos and P. Mehrkhodavandi, *Dalton Trans.*, 2015, **44**, 14248–14254; (g) L. E. Chile, P. Mehrkhodavandi and S. G. Hatzikiriakos, *Macromolecules*, 2016, **49**, 909–919; (h) L. E. Chile, T. Ebrahimi, A. Wong, D. C. Aluthge, S. G. Hatzikiriakos and P. Mehrkhodavandi, *Dalton Trans.*, 2017, **46**, 6723–6733.
- 19 (a) D. C. Aluthge, B. O. Patrick and P. Mehrkhodavandi, *Chem. Commun.*, 2013, **49**, 4295–4297; (b) D. C. Aluthge, E. X. Yan, J. M. Ahn and P. Mehrkhodavandi, *Inorg. Chem.*, 2014, **53**, 6828–6836; (c) D. C. Aluthge, J. M. Ahn and P. Mehrkhodavandi, *Chem. Sci.*, 2015, **6**, 5284–5292; (d) T. Ebrahimi, D. C. Aluthge, S. G. Hatzikiriakos and P. Mehrkhodavandi, *ACS Catal.*, 2017, **7**, 6413–6418.
- 20 H. J. Jung, C. Chang, I. Yu, D. C. Aluthge, T. Ebrahimi and P. Mehrkhodavandi, *ChemCatChem*, 2018, **10**, 3219–3222.
- 21 C. Diaz, T. Ebrahimi and P. Mehrkhodavandi, *Chem. Commun.*, 2019, **55**, 3347–3350.
- 22 A. Murphy, A. Pace and T. D. P. Stack, *Org. Lett.*, 2004, **6**, 3119–3122.
- 23 (a) U. Mayer, V. Gutmann and W. Gerger, *Monatsh. Chem.*, 1975, **106**, 1235–1257; (b) G. C. Welch, L. Cabrera, P. A. Chase, E. Hollink, J. D. Masuda, P. R. Wei and D. W. Stephan, *Dalton Trans.*, 2007, 3407–3414.
- 24 M. Sandstrom, I. Persson and P. Persson, *Acta Chem. Scand.*, 1990, **44**, 653–675.
- 25 K. E. Horner and P. B. Karadakov, *J. Org. Chem.*, 2013, **78**, 8037–8043.
- 26 F. Cataldo, *Eur. Chem. Bull.*, 2015, **4**, 92–97.
- 27 D. G. S. Quattrociochi, G. B. Ferreira, L. M. da Costa and J. W. D. Carneiro, *Comput. Theor. Chem.*, 2016, **1075**, 104–110.
- 28 P. Li and K. Y. Qiu, *J. Polym. Sci., Part A: Polym. Chem.*, 2002, **40**, 2093–2097.
- 29 K. Matyjaszewski and S. Penczek, *Macromol. Chem. Phys.*, 1981, **182**, 1735–1742.
- 30 Z. Liu, M. Torrent and K. Morokuma, *Organometallics*, 2002, **21**, 1056–1071.
- 31 (a) X. Liu, X. Shang, T. Tang, N. Hu, F. Pei, D. Cui, X. Chen and X. Jing, *Organometallics*, 2007, **26**, 2747–2757; (b) M. Normand, E. Kirillov, T. Roisnel and J.-F. Carpentier, *Organometallics*, 2012, **31**, 1448–1457; (c) X. Shang, X. Liu and D. Cui, *J. Polym. Sci., Part A: Polym. Chem.*, 2007, **45**, 5662–5672.

